

# CrystEngComm

Accepted Manuscript



This is an *Accepted Manuscript*, which has been through the Royal Society of Chemistry peer review process and has been accepted for publication.

*Accepted Manuscripts* are published online shortly after acceptance, before technical editing, formatting and proof reading. Using this free service, authors can make their results available to the community, in citable form, before we publish the edited article. We will replace this *Accepted Manuscript* with the edited and formatted *Advance Article* as soon as it is available.

You can find more information about *Accepted Manuscripts* in the [Information for Authors](#).

Please note that technical editing may introduce minor changes to the text and/or graphics, which may alter content. The journal's standard [Terms & Conditions](#) and the [Ethical guidelines](#) still apply. In no event shall the Royal Society of Chemistry be held responsible for any errors or omissions in this *Accepted Manuscript* or any consequences arising from the use of any information it contains.

Cite this: DOI: 10.1039/c0xx00000x

www.rsc.org/xxxxxx

ARTICLE TYPE

## Pressure-induced isostructural phase transition of a metal-organic framework $\text{Co}_2(4,4'\text{-bpy})_3(\text{NO}_3)_4 \cdot x\text{H}_2\text{O}$

Mi Zhou<sup>a,b</sup>, Kai Wang<sup>\*a</sup>, Zhiwei Men<sup>b</sup>, Chenglin Sun<sup>b</sup>, Zhanlong Li<sup>b</sup>, Bingbing Liu<sup>a</sup>, Guangtian Zou<sup>a</sup> and Bo Zou<sup>\*a</sup>

Received (in XXX, XXX) Xth XXXXXXXXX 200X, Accepted Xth XXXXXXXXX 200X  
DOI: 10.1039/b000000x

Based on 4,4'-bipyridine organic linker, metal-organic frameworks  $\text{Co}_2(4,4'\text{-bpy})_3(\text{NO}_3)_4 \cdot x\text{H}_2\text{O}$  (CB-MOF) have been prepared. The pressure-dependent structure evolution of CB-MOF has been investigated up to 11 GPa. An isostructural phase transition was concluded at about 6 GPa followed by negative compressibility for the *b* axis.

Metal-organic frameworks (MOFs) have attracted immense attention recently due to the possibility to obtain large variety of aesthetically interesting structures. They are formed by association of metal centers or clusters and organic linkers<sup>1</sup>. Most efforts are directed toward the synthesis of new frameworks with the largest possible surface areas, and the goal is to find exceptionally functional materials. These materials have displayed a large number of applications in many areas, such as adsorption, separation, and catalysis, which are based on the pore size and shape as well as the host-guest interactions involved<sup>2</sup>. The 4,4'-bipyridine ligand is one of the most reactive rod like organic linker to bridge metal centers to form one-, two-, and three-dimensionally frameworks<sup>3</sup>. And the transition-metal 4,4'-bipyridine complexes have powerful gas-adsorption properties<sup>3a,4</sup>.

During the past few years, some effort has been made to focus on the response of structures and properties of MOFs controlled by external parameters. Pressure is an important external stimulus that can cause changes in molecular geometry without the need to alter the material chemically, it can provide useful information in three important fields: (a) discoveries of new polymorphs and mechanisms of pressure-induced structural deformation, (b) the relationship between microporosity and compressibility and (c) structure-property correlation. Then the pressure response of MOFs has to be explored. And understanding the impact pressure on the coordination framework systems is not only for fundamental interest but is relevant to their practical applications. A few theoretical and experimental approaches have been devoted to the high-pressure behavior and pressure-induced structure evolution of microporous materials<sup>5</sup>, and some recent experiments have shown that the high-pressure behavior of microporous and mesoporous materials may be strongly influenced by the nature of the pressure transmitting medium (PTM)<sup>6</sup>. But to the best of our knowledge, no report about the pressure-induced isostructural phase transitions of MOFs is published. Hence, it is important to study the effect of pressure on MOFs structure, and there is clearly a need to understand the

structural response of MOFs to applied pressure.

In this communication, *in situ* Raman spectroscopy and angle dispersive X-ray diffraction (ADXRD) combined with symmetric diamond anvil cell (DAC) techniques have been conducted to study the structural stability of CB-MOF at high pressure. A detailed local structure evolution and isostructural phase transition of CB-MOF are concluded.

Raman spectroscopy is used to monitor the effect of pressure on the local structure of CB-MOF. The Raman peak positions are listed in Table S1 along with the appropriate vibrational assignments. The *in situ* Raman spectra of CB-MOF are acquired as a function of pressure up to 11 GPa at room temperature. The selected spectra are shown in Figure 1. The Raman frequency shift as a function of pressure are shown in Figure S1, the monotonous blue shift of the all Raman modes is observed up to 11 GPa, and we have not observed changes in the spectra including splitting of modes, appearance of new modes, or sudden changes in the slope of the frequency-pressure curve, so no obvious evidence of phase transition can be concluded during the entire compression processes.

As shown in Figure 1, it could be found that almost all the Raman peaks tend to broaden and weaken in intensity upon compressing. While, the relative intensity of 1621  $\text{cm}^{-1}$  band, which is attributed to the C-C stretching vibration ( $\nu_{8a}$ ) mode of the organic linker (4,4'-bipyridine), shows an intensity enhancement with pressure. Figure 2 displays the intensity ratio (1621  $\text{cm}^{-1}$  to 1022  $\text{cm}^{-1}$ )- pressure curve. The 1022  $\text{cm}^{-1}$  Raman band is attributed to ring breathing vibration ( $\nu_1$ ) mode. Based on linear curve fitting, below 6 GPa the slope is 0.1, while further

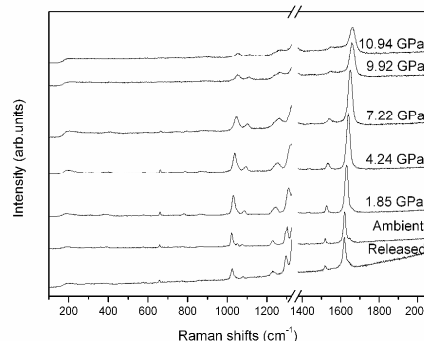
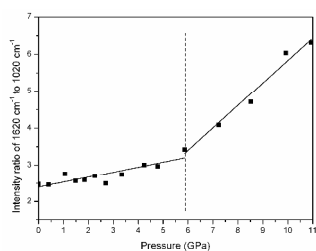


Fig.1 Selected high pressure Raman spectra of CB-MOF



**Fig.2** High pressure intensity ratio of 1620 $\text{cm}^{-1}$  to 1022 $\text{cm}^{-1}$

compression induce a remarkable intensity enhancement of 1621  $\text{cm}^{-1}$  Raman line, the slope is 0.6. Theoretical and experimental approaches show that the relative Raman intensities change is a test bench for probing the change in molecular structure from a nonplanar to a planar geometry of oligo-p-phenylenes<sup>7</sup>, e.g. for biphenyl, the calculated Raman intensity of 1770-1780  $\text{cm}^{-1}$  mode shows strong dependency with the twisting angle between two aromatic rings, the smaller twisting angle, the larger Raman intensity of C-C stretching band<sup>7a</sup>. For CB-MOF, the organic linker (4,4'-bipyridine) also posit a non-planar aromatic molecular geometry at ambient condition. Under compression, the much greater P-electron conjunctions in the planar molecular geometry induce the Raman intensity enhancement of C-C stretching ( $\nu_{8a}$ ) band. And the sudden slope change of relative intensity- pressure curve at 6 GPa may associate with higher-order phase transitions.

In order to know the coordination effect in MOFs at ambient condition, a comparative Raman spectra of 4,4'-bipyridine and CB-MOF are shown in Figure S2, and the exact peak positions are given in Table S1. It can be concluded that all the Raman bands blue shifted compared to the Raman spectrum of crystalline 4,4'-bipyridine. As a result of the direct coordination of the pyridine N to Co, the Raman shift of 1022  $\text{cm}^{-1}$  and 1621  $\text{cm}^{-1}$  bands, which are assigned to rings breathing mode ( $\nu_1$ ) and C-C stretching ( $\nu_{8a}$ ) mode respectively, have the largest frequency shifts and the  $\nu_{8a}$  band is the fundamental mode of Fermi resonance doublets, under compression, the Fermi resonance phenomenon is totally disappeared at 1 GPa.

To better understand the behavior of coordination effects in the coordination frameworks, an *in situ* high pressure Raman study of pure crystalline 4,4'-bipyridine solids was carried out in the same pressure range. The Raman spectra and Raman frequency shift as a function of pressure for the 4,4'-bipyridine crystal are shown in Figure S3 and S4. We also compare the frequency-pressure behavior of CB-MOF to 4,4'-bipyridine, the frequency-pressure slope of each Raman bands are listed in Table S1. Based on linear curve fitting, on the whole, the slope of the frequency-pressure curves of 4,4'-bipyridine are larger than that of its corresponding bands of MOFs, indicating the isolated molecule of organic linker endure more pressure in its crystalline than that in its metal-organic coordination architectures. And the metal-organic coordination networks play an important role in the volume reduction in the compression process. Because of lack of metal-organic coordination band in the Raman spectra of MOFs, the coordination effects under compression could be reflected from the changes in the frequency-relationship of the intra-molecular modes.

For comparison, an intensity-pressure curve of  $\nu_{8a}$  to  $\nu_1$  band (located at 1605 and 998  $\text{cm}^{-1}$  at ambient condition respectively)

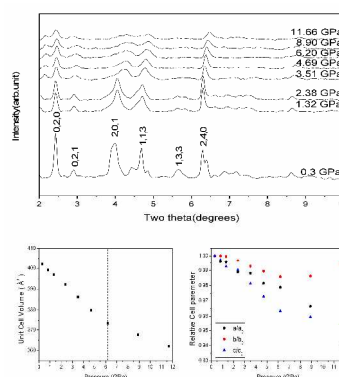


**Fig.3** Representative ADXRD patterns of CB-MOF, the unit cell volume as a function of pressure and anisotropic pressure response of the crystal lattices

of 4,4'-bipyridine is present in figure S5, in the pressure range from ambient up to 11 GPa, the intensity ratio increase from a value of 0.8 at ambient pressure to a value of about 1.6 at 11 GPa. The value and the slope of the intensity ratio for 4,4'-bipyridine is significant smaller than that of its MOFs, suggesting the electron-phonon coupling effect in crystalline 4,4'-bipyridine is much smaller than that of its MOFs, and the metal-organic architecture provides an specific environment for the pressure driven planar molecular geometry.

ADXRD was used to gain direct information on pressure-induced structural transformations. Representative ADXRD patterns of CB-MOF at various pressures are shown in Figure 3. As pressure increased, the peaks become broader and less intense and some merge together. From the ADXRD data, we can conclude that there is no obvious phase transition that occurred up to 11 GPa. Therefore, the high-pressure diffraction patterns can be indexed according to the orthorhombic unit cell.

Under ambient conditions, CB-MOF crystallizes into a orthorhombic structure with the *Ccca* space group,  $a=12.267(7)$ ,  $b=19.025(7)$ ,  $c=17.412(4)$  Å,  $V=4063(2)$  Å<sup>3</sup>. The pressure dependences of the unit cell volume and lattice parameters at room temperature are illustrated in Figure 3. As observed for many other molecular crystals<sup>8</sup>, the compressional behavior of CB-MOF is anisotropic, below 6 GPa, with the increase of pressure, it is evident that all the diffraction peaks shifted to higher angles, it can be seen that the b orientation is relatively stiff compared with the a and c orientations. When the pressure is raised above 6 GPa, the different nature and strength of interactions give rise to an anisotropic compression and, not surprisingly, the most compressed direction is the one corresponding to the weakest interaction, namely a, while the b axis shows a negative compressibility. So far, to the best of our knowledge, only one metal-organic framework material with negative compressibility has been reported<sup>9</sup>. From the high pressure Raman scattering and ADXRD results, no obvious first-order phase transitions could be concluded over the entire pressure range. While the relative intensity changes of C-C stretching Raman mode and the tendencies of pressure-induced lattice parameters changes suggesting that an isostructural phase transitions exist at about 6 GPa.

The evolution of the change in unit cell volume of CB-MOF as a function of pressure is shown in Figure 3. The indexed and refined structural parameters are given in Table S2. The volume

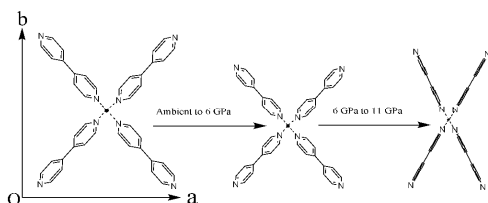


Fig.4 Scheme of pressure-induced structure change of CB-MOF

decreases with increasing pressure, as expected, and the measured percentage of shrinkage is about 1.0% per GPa. In the studied pressure range the bulk modulus of CB-MOF is estimated by using a second-order Birch-Murnaghan equation, Giving a value of  $K_0$  of 54.8 GPa. This value is significantly higher than those found for several zeolite imidazodate frameworks. According to the previous analysis about the local structure and lattice change of CB-MOF. A scheme of pressure-induced structure evolution of MOFs is proposed from the high-pressure Raman scattering and ADXRD results (Figure 4).

In summary, we report the high-pressure Raman and ADXRD measurements performed on CB-MOF, at various pressures up to 11 GPa. From the Raman frequency-pressure relationship, all the vibrational frequencies upshift linearly with pressure indicating that there is no obvious first-order phase transition during compression. While a pressure-induced intensity enhancement phenomenon is observed for C-C stretching mode, suggesting a planar molecular conformation of organic linker is present at high pressure. A comparative high-pressure Raman study of crystalline 4,4'-bipyridine is also conducted, the frequency-pressure slope of each Raman bands are larger than that of its metal organic frameworks, while the degree of pressure-driven Raman intensity enhancement effect of C-C stretching band in 4,4'-bipyridine is not so significant as that of MOFs. The high-pressure ADXRD diffraction data of MOFs suggest that an isostructural phase transition occurs at 6 GPa, at which pressure a negative compressibility is observed in b-axis direction.

The authors are grateful to Dr. Ho-kwang Mao for help on experiments. This work is supported by the NSFC (No.11104107 and 91227202), the National Basic Research Program of China (No.2011CB808200), National Found for Fostering Talents of basic Science (NO. J1103202). This work was performed at HPCAT's beamline facility of the Advanced Photon Source at Argonne National Laboratory. HPCAT is supported by CIW, CDAC, UNLV and LLNL through funding from DOE-NNSA, DOE-BES and NSF. APS is supported by DOE-BES (No. DE-AC02-06CH11357).

## Notes and references

<sup>a</sup> State Key Laboratory of Superhard Materials, Jilin university, Changchun, R. R. China. Fax: +86-431-85168883; Tel: X+86-431-85168882; E-mail: zoubu@jlu.edu.cn

<sup>b</sup> College of Physics, Jilin university, Changchun, R. R. China.

† Electronic Supplementary Information (ESI) available: Experimental details, table 1,2 and figures of 4,4'-bipyridine. See DOI: 10.1039/b000000x/

(a) H. Li, M. Eddaoudi, M. O'keeffe and O. M. Yaghi, *Nature*, 1999, **402**, 276-279; (b) E. D. Bloch, W. L. Queen, R. Krishna, J. M. Zadrozny, C. M. Brown and J. R. Long, *Science*, 2012, **30**, 1606-1610; (c) R. Chakrabarty, P. S. Mukherjee and P. J. Stang, *Chem. Rev.*, 2011, **111**, 6810-6918; (d) W. Zhang and R. Xiong, *Chem. Rev.*,

2012, **112**, 1163-1195; (e) S. M. Cohen, *Chem. Rev.*, 2012, **112**, 970-1000.

(a) A. Betard and R. A. Fischer, *Chem. Rev.*, 2012, **112**, 1055-1083; (b) A. R. Millward and O. M. Yaghi, *J. Am. Chem. Soc.*, 2005, **127**, 17998-17999; (c) J. Li, J. Sculley and H. Zhou, *Chem. Rev.*, 2012, **112**, 869-932; (d) D. Britt, H. Furukawa, B. Wang, T. G. Glover and O. M. Yaghi, *Proc. Natl. Acad. Sci. USA*, 2009, **106**, 20637-20640; (e) M. Yoon, R. Srirambalaji and K. Kim, *Chem. Rev.*, 2012, **112**, 1196-231.

(a) S. Noro, S. Kitagawa, M. Kondo and K. Seki, *Angew. Chem. Int. Ed.*, 2000, **39**, 2082-2084; (b) B. R. Bhogala, P. Vishweshwar and A. Nangia, *Cryst. Growth Des.*, 2002, **2**, 325-328; (c) J. Lu, T. Paliwala, S. C. Lim, C. Yu, T. Niu and A. J. Jacobson, *Inorg. Chem.*, 1997, **36**, 923-929; (d) D. M. S. Martins, D. S. Middlemiss, C. R. Pulham, C. C. Wilson, M. T. Weller, P. F. Henry, N. Shankland, K. Shankland, W. G. Marshall, R. M. Ibberson, K. Knight, S. Moggach, M. Brunelli and C. A. Morrison, *J. Am. Chem. Soc.*, 2009, **131**, 3884-3893; (e) K. Biradha, M. Sarkar and L. Rajput, *Chem. Commun.*, 2006, **40**, 4169-4179.

M. Kondo, T. Yoshitomi, K. Seki, H. Matsuzaka and S. Kitagawa, *Angew. Chem. Int. Ed.*, 1997, **36**, 1725-1727.

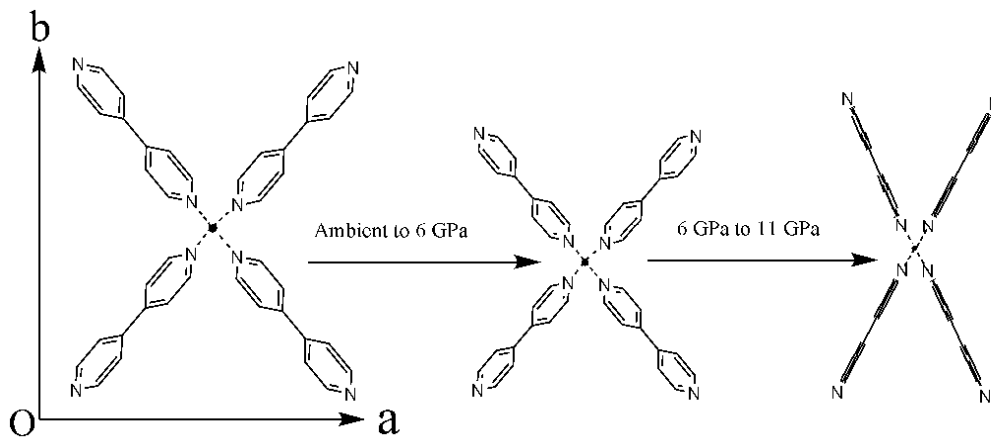
(a) S. A. Moggach, T. D. Bennett and A. K. Cheetham, *Angew. Chem. Int. Ed.*, 2009, **48**, 7087-7089; (b) I. Beurroies, M. Boulhout, P. L. Llewellyn, B. Kuchta, G. Frey, C. Serre and R. Denoyel, *Angew. Chem. Int. Ed.*, 2010, **49**, 7526-7529; (c) A. J. Graham, D. R. Allan, A. Muszkiewicz, C. A. Morrison and S. A. Moggach, *Angew. Chem. Int. Ed.*, 2011, **50**, 11138-11141; (d) Hoffmann, H. C. Assfour, B.; Epperlein, F.; Klein, N.; Paasch, S.; Senkovska, I.; Kaskel, S.; Seifert, G.; Brunner, E. *J. Am. Chem. Soc.*, 2011, **133**, 8681-8690; (e) E. C. Spencer, R. J. Angel, N. L. Ross, B. E. Hanson and J. A. K. Howard, *J. Am. Chem. Soc.*, 2009, **131**, 4022-4026; (f) K. W. Chapman, G. J. Halder and P. J. Chupas, *J. Am. Chem. Soc.*, 2009, **131**, 17546-17547; (g) K. W. Chapman, D. F. Sava, G. J. Halder, P. J. Chupas, T. M. Nenoff, *J. Am. Chem. Soc.*, 2011, **133**, 18583-18585; (h) J. L. Musfeldt, Z. Liu, S. Li, J. Kang, C. Lee, P. Jena, J. L. Manson, J. A. Schlueter, G. L. Carr and M. H. Whangbo, *Inorg. Chem.*, 2011, **50**, 6347-6352; (i) W. Li, M. R. Probert, M. Kosa, T. D. Bennett and A. Thirumurugan, R. P. Burwood, M. Parinello, J. A. K. Howard, A. K. Cheetham, *J. Am. Chem. Soc.*, 2012, **134**, 11940-11943; (j) Y. Huang and E. A. Havenga, *Chem. Phys. Lett.*, 2001, **345**, 65-71; (k) Y. Hu, H. Kazemian, S. Rohani, Y. Huang and Y. Song, *Chem. Commun.*, 2011, **47**, 12694-12696; (l) Y. Fu, Y. Song, Y. Huang, *J. Phys. Chem. C.*, 2012, **116**, 2080-2089; (m) P. Serra-Crespo, E. Stavitski, F. Kapteijn and J. Gascon, *RSC Adv.*, 2012, **2**, 5051-5053; (n) T. D. Bennett, P. Simoncic, S. A. Moggach, F. Gozzo, P. Macchi, D. A. Keen, J. Tan and A. K. Cheetham, *Chem. Commun.*, 2011, **47**, 7983-7985; (o) T. D. Bennett, A. L. Goodwin, M. T. Dove, D. A. Keen, M. G. Tucker, E. R. Barney, A. K. Soper, E. G. Bithell, J. Tan, and A. K. Cheetham, *Phys. Rev. Lett.* 2010, **104**, 115503; (p) Y. Hu and L. Zhang, *Phys. Rev. B.* 2010, **81**, 174103; (q) A. U. Ortiz, A. Boutin, A. H. Fuchs, and F. Coudert, *J. Phys. Chem. Lett.*, 2013, **4**, 1861-1865.

(a) K. W. Chapman, G. J. Halder and P. J. Chupas, *J. Am. Chem. Soc.*, 2008, **130**, 10524-10526; (b) S. A. Moggach, T. D. Bennett and A. K. Cheetham, *Angew. Chem. Int. Ed.*, 2009, **121**, 7221 - 7223; (c) Y. Lee, T. Vogt, J. A. Hriljac, J. B. Parise and G. Artioli, *J. Am. Chem. Soc.*, 2002, **124**, 5466-5475; (d) Y. Lee, T. Vogt, J. A. Hriljac, J. B. Parise, J. C. Hanson and S. J. Kim, *Nature*, 2002, **420**, 485-489.

(a) S. Guha, W. Graupner, R. Resel, M. Chandrasekhar, H. R. Chandrasekhar, R. Glaser and G. Leising, *Phys. Rev. Lett.*, 1999, **82**, 3625-3628; (b) S. Guha, W. Graupner, R. Resel, M. Chandrasekhar, H. R. Chandrasekhar, R. Glaser and G. Leising, *J. Phys. Chem. A.*, 2001, **105**, 6203-6211.

(a) K. Wang, D. F. Duan, M. Zhou, S. R. Li, T. Cui, B. B. Liu, J. Liu, B. Zou and G. T. Zou, *J. Phys. Chem. B.*, 2011, **115**, 4639-4644; (b) K. Lekin, A. A. Leitch, J. S. Tse, X. Bao, R. A. Secco, S. Desgreniers, Y. Ohishi and R. T. Oakley, *Cryst. Growth Des.*, 2012, **12**, 4676-4684

W. Li, M. R. Probert, M. Kosa, T. D. Bennett, A. Thirumurugan, R. P. Burwood, M. Parinello, J. A. K. Howard and A. K. Cheetham, *J. Am. Chem. Soc.*, 2012, **134**, 11940-11943.



**Highlighting the novelty of the work:** A pressure induced isostructural phase transition is found in a metal-organic framework  $\text{Co}_2(4,4'\text{-bpy})_3(\text{NO}_3)_4 \cdot x\text{H}_2\text{O}$